Mapping Snowpack Depth beneath Forest Canopies Using Airborne Lidar

Chris Hopkinson, Mike Sitar, Laura Chasmer, and Paul Treitz

Abstract

An evaluation of airborne lidar (Light Detection And Ranging) technology for snow depth mapping beneath different forest canopy covers (deciduous, coniferous, and mixed) is presented. Airborne lidar data were collected for a forested study site both prior to and during peak snowpack accumulation. Manual field measurements of snow depth were collected coincident with the peak snowpack lidar survey, and a comparison between field and lidar depth estimates was made. It was found that (1) snow depth distribution patterns can be mapped by subtracting a "bare-earth" DEM from a "peak snowpack" DEM, (2) snow depth estimates derived from lidar data are strongly related to manual field measures of snow depth, and (3) snow depth estimates are most accurate in areas of minimal understory. It has been demonstrated that airborne lidar data provide accurate snow depth data for the purpose of mapping spatial snowpack distribution for volume estimations, even under forest canopy conditions.

Introduction

Rationale

Knowledge of spring snowpack conditions is essential for the prediction of water availability and flood peaks following the onset of melt. Evaluating snowpack conditions in forest regions is particularly important because the canopy cover influences accumulation and melt processes and, therefore, has a marked effect on the downstream hydrograph (e.g., Elder *et al.,* 1998). Current ground-based snow depth measurements are manually intensive, limited in spatial extent, and generally costly in remote areas. In addition, manually assessing snowpack depth distribution under forest canopies can be difficult due to heterogeneous ground and understory conditions (Adams and Barr, 1970). There is a strong justification, therefore, for investigating remote techniques of snowpack distribution measurement in such areas. Recently, Derksen *et al.* (2001) demonstrated that passive microwave technology is useful for estimation of snow water equivalent (SWE) in forest regions. However, such methods are unreliable for dense canopies and during snowmelt (Derksen *et al.*, 2001), and the spatial resolution is too low to assess snowpack conditions at the individual forest stand scale. This paper presents an evaluation of high-resolution airborne lidar technology for the application of spatial snow depth mapping within conifer and deciduous forest stands.

C. Hopkinson and L. Chasmer are with Otterburn Geographic, 387 Nelson St., Kingston, ON K7K 4M9, Canada and the Laboratory for Remote Sensing of Earth and Environmental Systems, Department of Geography, Queens University, Kingston, ON K7L 3N6, Canada (chopkinson@cogeco.ca; lechasme@yahoo.ca).

M. Sitar is with Optech Inc., 100 Wildcat Rd., Toronto, ON M3J 2Z9, Canada (michaels@optech.on.ca).

P. Treitz is with the Laboratory for Remote Sensing of Earth and Environmental Systems, Department of Geography, Queens University, Kingston, ON K7L 3N6, Canada (pt6@qsilver.queensu.ca).

Airborne Lidar

Due to continual advances in lidar technology, lasers are increasingly being adopted to accurately measure distances. Airborne lidar (also referred to as laser altimetry) combines (1) a knowledge of the speed of light, (2) the location of the laser head in space, and (3) the time from laser pulse transmission to reception in order to determine a three-dimensional coordinate on the ground. Utilizing standard scanning technology, laser pulses are swept left and right, perpendicular to the line of flight, resulting in a "saw tooth" pattern of surveyed points on the ground. The resultant data can be used to create a high-resolution (sub-meter) digital terrain model of the ground surface. To ensure that the data collected represent actual ground conditions, it is necessary to reference the laser head (from which the laser pulse is emitted) to known control points on the ground. This is achieved using differential GPS, whereby at least one survey grade GPS receiver and antenna is located over a known control point (generally within 50 km of the survey area) and another is located inside the aircraft. Through postprocessing of the aircraft GPS trajectory, the location of the laser head is continually fixed in space. The quality of the final data product is largely related to the accuracy of the GPS trajectory. Further refinement of the trajectory and compensation for aircraft attitude variation (i.e., pitch, roll, and yaw) is achieved by postprocessing data collected by an onboard inertial navigation system (INS). Current technology can collect multiple returns at pulse repetition frequencies (PRF) up to 75 kHz. The resultant laser spot spacing on the ground can be as low as 30 cm in both the X and Y directions, and the ground swath typically varies between 0 and 2000 m depending on flying altitude and scan angle. For more information, see Gutelius (1998) and Baltsavias (1999).

Airborne lidar is becoming increasingly popular for a variety of biogeophysical applications, e.g., forest structure and inventory (St-Onge *et al.*, 2000; Means *et al.*, 2000; Lim *et al.*, 2001; Lim *et al.*, 2003), glaciology (Kennet and Eiken, 1997; Hopkinson *et al.*, 2001), icesheet thickness change detection (Krabill *et al.*, 1995), radiation loading scaling issues (Chasmer and Hopkinson, 2001), and others ranging from shoreline degradation to hydro wire damage in remote regions (Flood and Gutelius, 1997). In addition, the cost effectiveness of airborne lidar over traditional manually intensive field techniques for flood mapping and environmental change detection has been demonstrated by Holden (1998).

Photogrammetric Engineering & Remote Sensing
Vol. 70, No. 3, March 2004, pp. 323–330.

0099-1112/04/7003–0323/$3.00/0

Study Area

The North Tract of York Regional Forest (Figure 1) is approximately 50 km north of Toronto in southern Ontario, Canada and was selected for this study for a variety of reasons. Most importantly, the site lies on the flight path used by Optech Inc. (a Canadian airborne lidar manufacturer) for their routine Airborne Laser Terrain Mapper (ALTM) system calibrations. Thus, the required surveys could be incorporated into Optech's flight-testing schedule on a "window of opportunity" basis. In addition, a local silvicultural consultancy, Silv-Econ, manages these forest sites, and their GIS layers of forest inventory data and aerial photographs of the area were available for this study.

The study area overlies an undulating glacial till lithology and displays vegetation types similar to other managed forests in the region. The survey polygon illustrated in Figure 1 covers approximately 2.4 km^2 (2 km by 1.2 km). The forest stands investigated were all contained within a study area of 600 m by 600 m. The study site covers an elevational range of around 30 m and displays a variety of common canopy and ground-cover characteristics over a relatively small area. Three different forest stand types, common in the southern Ontario geographical context, were compared:

- Mature single-tier conifer plantation dominated by red (*Pinus resinosa*) and white (*Pinus strobus*) pines with trees over 20 m in height (73 percent of the study site) and no understory,
- Mature deciduous stand dominated by sugar maple (*Acer saccharum*) with trees up to 30 m in height (20 percent of study site) and a layer of brush at ground level, and
- Mixed young coniferous and deciduous stand. This area was clearcut in 1990 and has not been managed since. It is in an abandoned state at present with a multi-tiered and dense canopy of up to 4 m in height. (less than 7 percent of the study site).

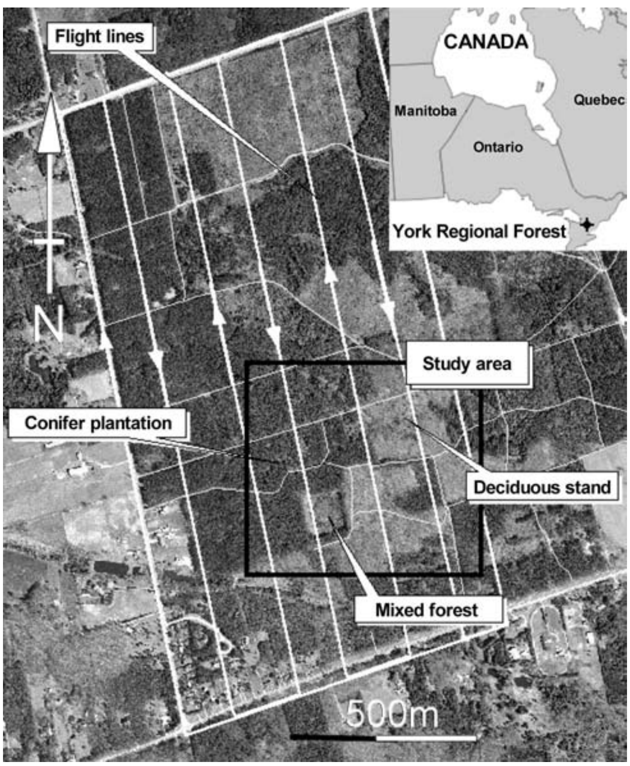

Figure 1. Aerial photograph acquired during fall 1999 of the York Regional Forest North Tract in southern Ontario, Canada. The three forest stands investigated are located within the black outline. The white lines illustrate the flight plan for the December survey.

Methods

Airborne Lidar Survey

Two airborne lidar surveys were performed over the study site: the first on 11 December 2000 during deciduous leaf off conditions prior to snow accumulation, and the second on 19 February 2001 prior to the onset of snow melt (see Figure 2a for a typical flight configuration). Both surveys were carried out by Optech Inc. The ALTM 1210 and ALTM 1225 (Figure 2b) were used for the December and February flights, respectively. Both systems utilize a 1064-nm wavelength scanning lidar with an industry quoted 15-cm standard deviation of absolute vertical error and a horizontal standard deviation of 1/2000 of the flying height. The main difference between the ALTM 1210 and 1225 is the maximum PRF; 10 kHz and 25 kHz, respectively.

Flight and sensor parameters (Table 1) for the December survey were optimized for high resolution and vegetation canopy penetration. Optimal parameters could not be implemented for the February survey due to limited sensor availability at the time of peak snowpack. A wide scan angle was adopted, making canopy penetration less effective (penetration is maximized at near-nadir scan angles). In Table 1 it can be seen that the ground spacings in *X* and *Y* for both surveys were almost equivalent despite different scan settings. This was due to the compensating effect of the ALTM 1225's higher PRF. The total survey times for the polygon in Figure 1 were approximately 30 and 10 minutes using the ALTM 1210 and 1225, respectively.

Lidar Processing and Snow Surface DEM Generation

The lidar data were combined with the GPS and INS data to generate *XYZ* data files of first- and last-pulse returns. In theory, this allows the simultaneous collection of both canopy and ground surface points. In addition, the data were classified as either ground or vegetation returns using Optech's "in-house" vegetation classification algorithm (within the Realm® software suite), which uses an iterative windowed spatial filtering technique to classify the points. This classification procedure was applied to both survey data sets to remove the influence of vegetation so that the December ground surface could be compared directly with the February snowpack surface. Each data set was gridded to a 1-m raster matrix (using an "inverse distance" interpolator) to facilitate DEM intercomparison and volumetric calculations. A 1-m resolution was chosen to slightly oversample the raw data density in an effort to maintain point integrity.

For the December survey, the GPS trajectory RMS errors were below 3 cm over the survey polygon. Unfortunately, the February airborne GPS data displayed several missing epochs

TABLE 1. LIDAR SURVEY INPUT AND OUTPUT PARAMETERS FOR THE DECEMBER AND FEBRUARY FLIGHTS

Input		Output	
Fall (December) Survey			
Repetition rate	10 kHz	*X* spacing	1.3 m
Scanner frequency	21 Hz	*Y* spacing	1.0 m
Scan angle	±10 deg	Footprint	0.2 m
Aircraft velocity	55 ms^{-1}	Swath width	250 m
Flying altitude	700 m a.g.l.		
Line spacing	200 m		
Winter (February) Survey			
Repetition rate	25 kHz	*X* spacing	1.1 m
Scanner frequency	28 Hz	*Y* spacing	1.2 m
Scan angle	±20 deg	Footprint	0.2 m
Aircraft velocity	60 ms^{-1}	Swath width	550 m
Flying altitude	750 m a.g.l.		
Line spacing	400 m		

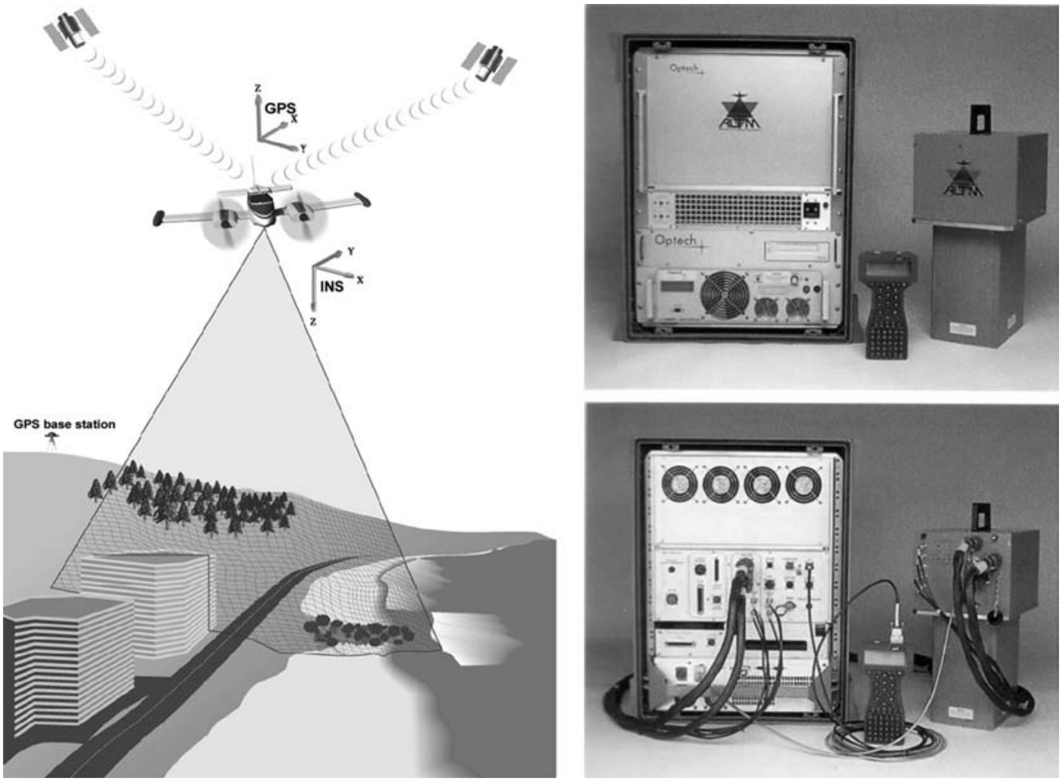

(a) (b)

Figure 2. (a) Diagram of aircraft, sensor, and GPS configuration. (b) Photographs of the ALTM 1225 system used during the February survey. (Images courtesy of Optech Incorporated.)

(gaps in raw GPS files) and this led to overall trajectory RMS errors between 10 cm and 1 m. As a result, the *XYZ* positions calculated for the February snowpack surface are not as reliable. However, the calibrations of both sensors were well within specification, and there were no apparent shifts or anomalies in the relative positioning of raw data. It was therefore necessary to co-register the two data sets using ground control. For small lidar data sets of this nature (i.e., internally sound but with a potential systematic bias), registration is simple and all that is needed is a single "tie point." Solid building edges in the southern portion of the survey polygon were adequate for this task. Due to the less reliable GPS data of the second survey, it was found necessary to shift the February DEM approximately 1 m to the west. Following rasterization and registration of the lidar data, it was then possible to subtract the December DEM from that of February to assess the spatial variability of snowpack depth and calculate the overall snow cover volume.

Ground-Based Data Collection

Three days prior to the February lidar survey, seven transects of snow depth measurements were recorded within the study site. (The ground and airborne surveys did not coincide due to low cloud conditions. However, cool temperatures with no precipitation during the intervening days ensured minimal alteration of the snowpack.) Snow depth validation data were only collected from three forest stands because it was not possible to sample all forest areas covered by the lidar surveys due to logistic time constraints, access restrictions, and challenging ground conditions, making movement and measurement difficult. Three sets of transect measurements were made in the deciduous stand; two ran parallel to one another, while a third ran across the stand, almost perpendicular to the first two. Within the conifer plantation, two perpendicular transects were traversed near the center of the stand. Snow depth data were also collected along two perpendicular transects across the mixed forest plot.

For six of the seven transects, measurements were made at approximately 10-m intervals. At all depth sample locations, the position was flagged with fluorescent tape and a nested measurement procedure was adopted, whereby depth readings were made in a diamond shape radiating out 1 m from a central point along the transect. These manual measurements were then averaged for each sample location. To register the ground-based depth measurements with the lidar data, a Trimble Pro XRS DGPS backpack system was subsequently taken into the field to survey in the previously flagged measurement locations. The average depth measurements collected on the ground were then compared with the average of corresponding nested raster grid nodes on the "difference" surface derived by subtracting the February from the December DEM. These two depth data sets were then compared and regressed to assess the level of correspondence.

Results and Discussion

Lidar Data

The high resolution DEM for the study area derived from the December data is presented in Figure 3. Individual trees, rows of trees, and pathways are visible in the shaded relief DEM containing the last-pulse lidar data (Figure 3a). The DEM image to the right (Figure 3b) has had all vegetation removed using the classification algorithm. For the December survey, the last-pulse penetration rate was 70 percent. This would indicate

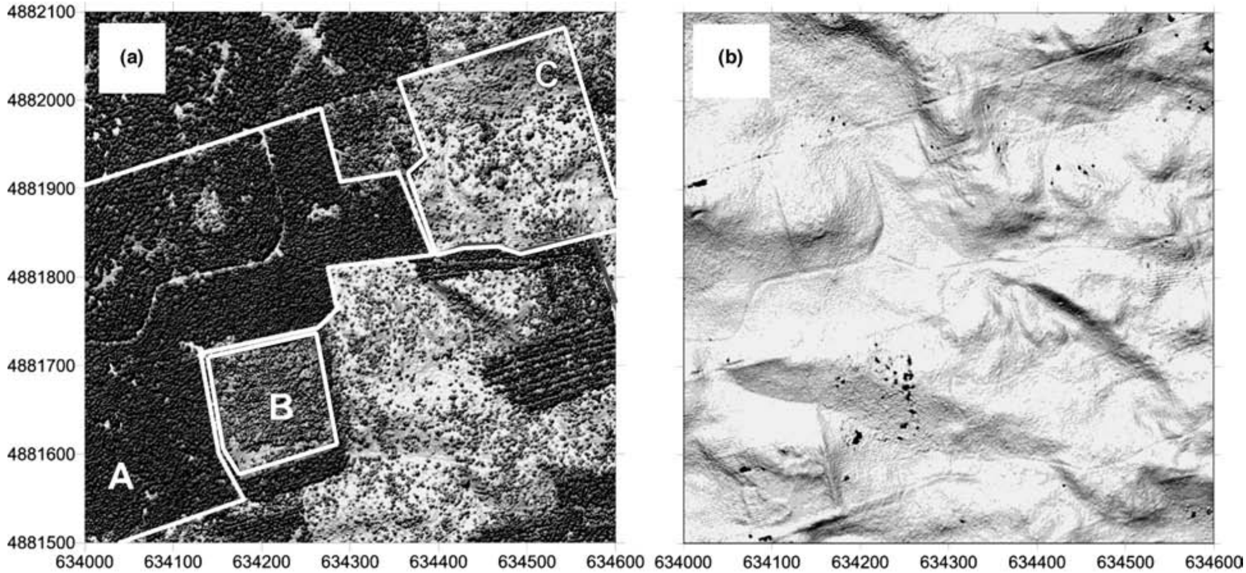

Figure 3. Shaded relief images of the December lidar survey (using the ALTM 1210 sensor) of the study area (UTM coordinate axes). To the left (a) is the 1-m rasterized lidar surface of all last pulse data, and to the right (b) is the 1-m vegetation-removed image. Forest stands investigated are labelled A: mature conifer plantation; B: young mixed forest; C: mature deciduous stand.

that, for every ten last-pulse returns, approximately three represent vegetation and seven represent ground. To put it another way, the average ground spacing was between 1.5 and 2 m in X and Y. However, the canopy conditions were variable and therefore the penetration rate also varied across the survey area. Comparative penetration statistics were not available for each of the forest stands, but it was assumed that ground spot spacing rarely exceeded 2 m because as the "inverse distance" rasterization procedure (see Golden Software, 1995) with a 1-m search radius produced only a few blank cells in the ground DEM (Figure 3b). For the February survey, the average penetration rate was 39 percent. This led to a spot spacing similar to that of December due to the higher PRF of the ALTM 1225. However, the ground returns were preferentially located near nadir angles due to higher proportions of vegetation hits at wider angles. Thus, despite the higher PRF on the 1225, the wider scan used in the February survey reduced the number of hits over the snowpack. Again, based on the rasterization procedure, ground spot spacings rarely exceeded 2 m over most of the survey area.

Lidar-Derived Snowpack Depth and Volume

The difference image derived from the 1-m gridded ground-cover DEMs for December and February is presented in Plate 1, and the statistics are provided in Table 2. Although the range of snow depth values (as inferred from the ground DEM subtraction) was greater than 3 m, it is apparent that 50 percent of the depth values were between 31 and 51 cm with a mean of 41 cm. The negative values are attributed to erroneous data points in one or the other of the survey sets, and are of little significance due to the computed negative volume constituting less than 0.1 percent of the positive snowpack volume.

There are some small areas (e.g., locations 1 and 2 on Plate 1) with lidar DEM depth estimates of greater than 1 m. It is suspected that these do not reflect true snowpack conditions for the following reasons:

Site 1—The linear feature alongside the footpath was the result of selective logging between the two surveys. Several conifers had been felled and piled in this area along the

Table 2. Surface Difference Statistics after Subtracting the December Ground DEM from that of February

Surface Difference	(cm)	Volume	(m^3)
Maximum	285	Positive	146530
Minimum	−81	Negative	27
Average	41		
Median	41	**Number of cells** =	354770
Standard deviation	17		
25th percentile	31		
75th percentile	51		

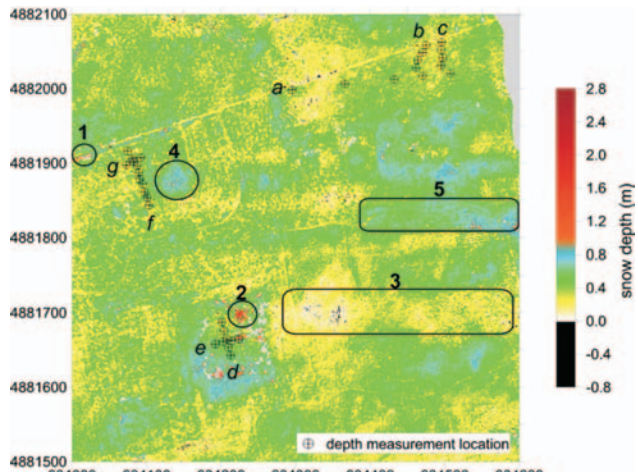

Plate 1. Map of the transect sample locations overlain onto a snowpack depth surface image generated by subtracting the December bare-earth DEM from the February (peak snowpack) DEM. Features 1 through 5 are discussed in the text.

path. Snow accumulated on the logs causing an apparently higher ground surface than actually existed;
Site 2—At this location there was a collection of densely packed immature conifers of less than 4 m in height. In December, some of the lidar pulses penetrated to the ground but during February, heavy snow accumulation on the low-lying canopy shielded the ground from view, and the vegetation classification algorithm interpreted the ground as lying within the canopy.

As with the negative depth values, the areas displaying depths greater than 1 m did not lead to a significant snow depth estimation error, because they constituted around 1 percent of the total positive volume. For depths greater than 75 cm, the volume contribution was around 5 percent.

Assuming that the difference between the December and February ground surface DEMs was due to snowpack variability, then the effects of land cover and topography on snow depth should be evident. Plate 1 suggests that snow depth was widely variable and it therefore needed to be determined whether or not these variations were commensurate with known distribution patterns. A qualitative assessment of the patterns visible in Plate 1 provided several observations:

- Snowpack was deeper in forested clearings than beneath the adjacent canopy (area 4);
- Snowpack was shallow on ridge tops and deep in valley bottoms (areas 3 and 5);
- Snowpack tended to be deeper and more variable in the deciduous stand;
- Topography dominated snow depth variability in open areas, with canopy closure dominating in conifer plantations (confirmation that such patterns would be expected in this kind of environment is provided in McKay and Gray (1981) and Adams and Barr (1979));
- Snow depth along footpaths was lower than in adjacent areas (due to trampling); and
- Snow accumulation was deeper around the inside edge of the mixed forest area, and there were areas where depth diminished with distance from footpaths. These edge effects were possibly due to wind induced drifting and deposition (e.g., Goodison *et al.*, 1981)

These general observations tend to be in agreement with current knowledge of snowpack distribution patterns (for example, MacKay and Gray (1981)).

Comparison of Lidar-Derived and Manual Snow Depth Estimates

Due to dense canopy and subsequent errors related to GPS signal multipath conditions within the forest, the ground GPS positions of the manual snow depth measurements displayed horizontal RMS errors of approximately 2 m. Therefore, there is some uncertainty surrounding the exact correspondence of manual and lidar-based depth estimates. However, given that each manual and lidar-based measurement was nested and averaged over an area of approximately 2 m by 2 m, errors related to positional uncertainty have been minimized. Comparative depth statistics are provided in Table 3 and linear regression plots are illustrated in Figure 4.

Figure 4 demonstrates reasonable correspondence between the lidar-derived snow depth estimates and the manual measurements. For the average depth measurements at all sample locations, the coefficient of determination was 0.52, illustrating a weak relationship. However, this relationship was significant at the 99 percent confidence level ($P = 0.000002$). The strongest relationship was found in the conifer stand ($r^2 = 0.84$), and this was also significant at the 99 percent confidence level ($P = 0.00003$). Both the deciduous and mixed forest plots demonstrated very weak relationships ($r^2 = 0.4$), and neither of these were significant at the 99 percent confidence level.

The summary statistics in Table 3 provide a quantitative comparison of manual and lidar-derived depth measurements. The main observations were that lidar-derived depth estimates demonstrated greater ranges and variability, and for the deciduous and mixed plots, the estimated depths were systematically lower. The average difference between all lidar estimates and manual measurements was 6 cm (or around 15 percent of total snowpack volume), but this was largely due to an apparent systematic underestimation of snow depth in the deciduous stand of 13 cm. In the conifer stand the manual and lidar-derived depth estimates were within 1 cm of each other. This suggests, therefore, that some characteristic of the deciduous stand has led to a systematic lowering of the lidar depth estimate. This could occur if, in the area of the deciduous stand depth measurements, the February DEM was underestimated or if the December DEM was overestimated. Given that the snowpack surface was highly reflective and relatively smooth compared to the underlying ground surface, it would be more logical to assume that the bare-earth DEM collected in December was in error. Therefore, it would appear that, despite reduced canopy cover (relative to the other two site types investigated), the systematic underestimation of snow depth in the deciduous stand was related to the lidar ground-return data collected in December.

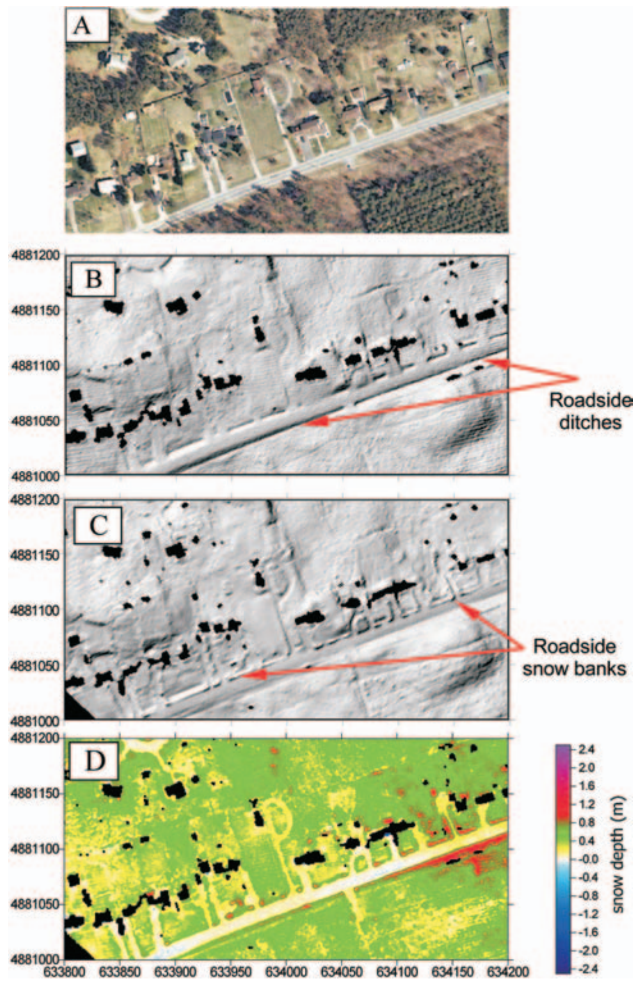

Plate 2. Residential area 1 km south of study site. A: aerial photograph collected during fall 1999; B: shaded relief image of rasterized ALTM data, December 2000; C: shaded relief ALTM data, February 2001; D: February–December DEM illustrating snowpack depth map. Black areas correspond to buildings or large objects removed using vegetation classification algorithm.

Table 3. Statistical Summary of Raw Snow Depth Measurements (Four to Five Manual Readings at each Sample Location) and Lidar-Derived Depth Estimates (Five Pixels at each Sample Location)

Manual Field Snow Depth Measurements				
Statistics	Deciduous	Conifer	Mixed	Overall
mean	44	33	51	42
min	29	12	23	12
max	59	60	64	64
25th percentile	39	25	46	35
75th percentile	47	42	57	49
std dev	6	13	9	12
Number	65	48	37	150
Lidar-Based Snow Depth Estimates				
Statistics	Deciduous	Conifer	Mixed	Overall
mean	31	34	46	36
min	12	8	7	8
max	57	60	68	68
25th percentile	26	24	37	27
75th percentile	38	43	54	45
std dev	11	15	13	13
Number	65	60	45	170

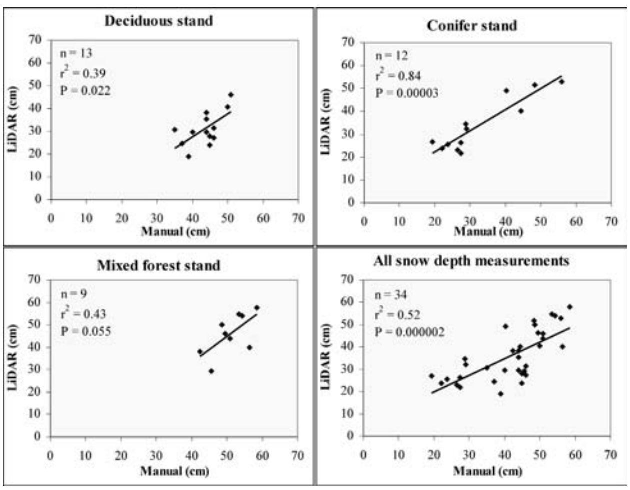

Figure 4. Regression plots of average manual snow depth measurements with average lidar DEM subtraction estimates for each transect sample location.

Ground Covers

The differences in estimated snow depth reliability for each forest type can likely be attributed to different ground covers. Figure 5 illustrates the common ground covers encountered in the deciduous and conifer stands. The ground cover and understory of the mixed forest stand cannot be easily distinguished from the canopy due to the densely packed and immature nature of the trees. The differences in ground cover and understory vegetation between the conifer and deciduous stands could affect lidar snow depth estimates in the following ways:

- The deciduous stand has a dense and varied understory of shrubs and immature trees, through which only a fraction of the laser footprint can penetrate. The implication of this observation is that a high proportion of last-pulse returns are from within the understory and not the ground surface. The net result of the understory would therefore be a systematic overestimation of the lidar ground surface height. The same difficulties should be minimal for the snow surface given that it is elevated above and more highly reflective than the bare-earth ground surface. Hence, as observed here, the lidar-derived snowpack depth for the deciduous stand would therefore be systematically underestimated.
- The conifer plantation generally had no understory. The flat and opaque nature of the pine needle mat at ground level provides a good surface for lidar returns, and thus the average ground elevation predicted from airborne lidar measurements should represent the actual ground surface to which snow would settle. There was, therefore, little likelihood of a similar systematic underestimation of lidar-derived snow depth.

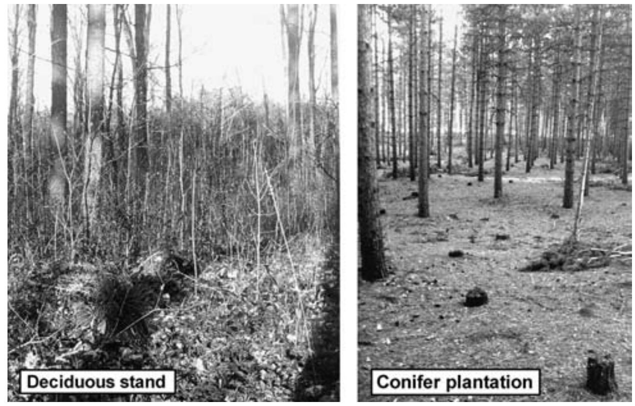

Figure 5. Ground cover beneath forest canopies for sugar maple (*Acer saccharum*) and red pine (*Pinus resinosa)* stands during late fall.

These results demonstrate that canopy understory can cause systematic biases in ground surface height and snow depth estimates from airborne lidar data. With further investigation of systematic lidar elevation biases associated with ground cover, it may be possible to assign type-dependent elevation offsets to improve elevation and snow depth estimates.

Application of Lidar Snow Depth Mapping

The analysis and discussion thus far have provided quantitative evidence for the utility of airborne lidar for spatial snow depth mapping over difficult ground cover and beneath different canopy types. However, this evidence is limited in spatial extent and may even appear somewhat esoteric for those with little appreciation of snowpack distribution behavior within forest environments. Perhaps visually more compelling evidence is provided in Plate 2, where the area used for registering the two lidar data sets is illustrated. From the aerial photo ("A" in Plate 2), it is apparent that this area is rural residential with a paved road running across the bottom of the image. From the difference DEM ("D" in Plate 2), several features are apparent that are clearly related to snowpack. Most prominently, the road and most driveways demonstrate the shallowest snow depths (±10 cm along the paved road) due to snow clearing operations. The deepest snow depths are evident in naturally filled roadside ditches and along driveway/roadside snow banks, also caused by snow ploughing. The average depth of snow in this scene was found to be 42 cm (virtually identical to that estimated for the forest areas) but the standard deviation was slightly higher at 21 cm (compared to 17 cm), probably due to the anthropogenic snow redistribution processes.

With appropriate estimates or supplemental measurements of snow density, the snowpack volumes measured in such residential and forest covered areas could be converted to an estimate of water equivalent, thus enabling the rapid assessment of end of winter snowpack water storage within heterogeneous basins. However, given the current high price of commercial lidar surveys, this method of snowpack surveying would be uneconomical in most situations. One environment that could potentially benefit from the application of this technique is in mountainous areas where snowpack depth tends to be high at the end of winter (thus reducing the influence of Lidar and ground cover errors) and where manual snowpack assessments are difficult and costly.

In North America, forested mountain areas are often the headwaters of rivers that flow into arid prairie regions and, as such, snowpack data are essential for regional annual water resource predictions. For example, the Bow River in Alberta, Canada rises in the Rocky Mountains and flows eastward into heavily irrigated prairie lands. Each year, helicopter snow surveys are employed between four and six times during winter months to assess basin-wide snow water equivalent at approximately 12 sites (Alberta Environmental Protection, 2000). Assuming that this task requires two field technicians and approximately 2½ hours of helicopter time for each day of snow surveys, the annual cost of this task amounts to approximately US$12,000 (Allison, personal communication, 2002). For the same price, a one-day commercial airborne lidar survey could be mobilized to collect data over approximately 12,000 acres (50 km^2) (Airborne One, personal communication, 2002). Although a lidar data collection campaign has limited temporal coverage (and requires a pre snowpack DEM), it gains substantially in terms of spatial coverage. In time, lidar surveys will become more economical, thereby making it feasible for water resource managers to consider this technology for future monitoring programmes.

Concluding Remarks

This paper has evaluated the utility of high-resolution airborne lidar technology for the purpose of snowpack depth mapping and volume estimation under various forest canopy types. The study presented here faced challenges due to the relatively shallow average snowpack depth of between 25 and 50 cm being little more than two to three times the quoted accuracy of the ALTM instruments. In addition, logistical difficulties were encountered with regard to survey timing and optimal parameter settings. However, despite these challenges, the following conclusions can be made:

- Lidar-derived ground DEMs for pre and peak snow cover periods can be compared to generate a "difference" surface characteristic of realistic snowpack distribution patterns, with observed variability commensurate with topographic and canopy closure controls.
- There is a statistically significant relationship between lidar-derived snow depth estimates and manual field measurements. This relationship is strongest for the conifer plot and weakest for deciduous stands with a dense understory.
- Canopy understory conditions have been found to introduce a systematic error in airborne lidar snow depth estimation within the deciduous stand. With *a priori* knowledge of ground-cover conditions, however, such errors could be reduced using a correction factor specific to certain ground/canopy types. There is, therefore, a need to assess the value of such systematic errors for different ground-cover types.

In summary, this paper has demonstrated that airborne lidar is potentially useful for snow-depth mapping in forest-covered regions. The utility of this technology would be greatest in areas prone to deep snowpack conditions, where instrument precision becomes less important, and over remote regions where ground access is difficult and costly. In most areas, the bare-earth data set would only need to be collected once, and in subsequent years monitoring would only require one survey near the end of winter. Considering that high-resolution survey data for areas of 100 km^2 can be collected in less than one hour (e.g., Holden, 1998; Hopkinson *et al.*, 2001), it is plausible that where manual data collection is difficult and costly, such as in the Rocky Mountains, lidar snowpack surveys may soon provide an economical supplement or even an alternative to traditional techniques.

Acknowledgments

Mr. Len Munt, York Regional Forester, for allowing the use of the Vivian Forest North Tract for this study; Chris Gynan of Silv-Econ Ltd. for providing raw forest coverage data and assistance in the field; and members of the 3rd year "Drainage Basin Ecosystems" class at Wilfrid Laurier University for assisting with field data collection.

References

Adams, W., and D. Barr, 1979. Vegetation-snow relationships in Labrador, *Proceedings of the Eastern Snow Conference, 36th Annual Meeting*, Alexandria Bay, New York, pp. 1–25.

Alberta Environmental Protection, 2000. *Snow Survey Report for the Bow River Basin, Alberta, Canada*, Alberta Environmental Protection, Edmonton, Alberta, Canada, one-page spreadsheet.

Baltsavias, E.P., 1999. Airborne laser scanning: Basic relations and formulas, *ISPRS Journal of Photogrammetry and Remote Sensing*, 54:199–214.

Chasmer, L., and C. Hopkinson, 2001. Using airborne laser altimetry and GIS to assess scale induced radiation-loading errors in a glacierised basin, *Proceedings of the 58th Eastern Snow Conference*, 14–18 May, Ottawa, Ontario, Canada, pp. 195–205.

Derksen, C., E. LeDrew, A. Walker, and B. Goodison, 2001. Evaluation of the Meteorological Service of Canada Boreal Forest snow water equivalent algorithm, *Proceedings of the 58th Eastern Snow Conference*, 14–18 May, Ottawa, Ontario, Canada, pp. 249–252.

Elder, K., W. Rosenthal, and R. Davis, 1998. Estimating the spatial distribution of snow water equivalence in a montane watershed, *Hydrological Processes*, 12:1793–1808.

Flood, M., and B. Gutelius, 1997. Commercial implications of topographic terrain mapping using scanning airborne laser radar, *Photogrammetric Engineering & Remote Sensing*, 63:327–366.

Golden Software Inc., 1995. *Surfer® for Windows, Version 6: User's Guide*, Golden Software Inc., Golden, Colorado.

Goodison, B.E., H.L. Ferguson, and G.A. McKay, 1981. Measurement and data analysis, *The Handbook of Snow; Principles, Processes, Management and Use* (D.M. Gray and D.H. Male, editors), Pergamon Press, Toronto, Ontario, Canada, pp. 191–274.

Gutelius, W., 1998. Engineering/applications of airborne scanning lasers: Reports from the field, *Photogrammetric Engineering & Remote Sensing*, 64:246–253.

Holden, N., 1998. *Airborne LiDAR Feasibility Study*, Research and Development Technical Report No. TR E43, United Kingdom Environment Agency.

Hopkinson, C., M.N. Demuth, M. Sitar, and L.E. Chasmer, 2001. Applications of airborne LiDAR mapping in glacierised mountainous terrain, *Proceedings of the International Geoscience and Remote Sensing Symposium*, 09–14 July, Sydney, Australia, on CD ROM.

Kennet, M., and T. Eiken, 1997. Airborne measurement of glacier surface elevation by scanning laser altimeter, *Annals of Glaciology*, 24:235–238.

Krabill, W.B., R.H. Thomas, K.C. Jezek, K. Kuivinen, and S. Manizade, 1995. Greenland Ice Sheet Thickness Changes Measured by Laser Altimetry, *Geophysical Research Letters*, 22:2341–2344.

Lim, K., P. Treitz, A. Groot, and B. St-Onge, 2001. Estimation of individual tree heights using LiDAR remote sensing, *Proceedings of the 23rd Canadian Symposium on Remote Sensing*, 20–21 August, Sainte-Foy, Quebec, Canada (Canadian Remote Sensing Society), pp. 251–258.

Lim, K., P. Treitz, M. Wulder, B. St-Onge, and M. Flood, 2003. LiDAR remote sensing of forest structure, *Prog. Phys. Geog.*, 27:88–106.

McKay, G.A., and D.M. Gray, 1981. The distribution of snowcover, *The Handbook of Snow; Principles, Processes, Management and Use*, (D.M. Gray and D.H. Male, editors), Pergamon Press, Toronto: Ontario, Canada, pp. 153–189.

Means, J., S. Acker, B. Fitt, M. Renslow, L. Emerson, and C. Hendrix, 2000. Predicting forest stand characteristics with airborne scanning lidar, *Photogrammetric Engineering & Remote Sensing*, 66:1367–1371.

St-Onge, B., J. Dufort, and R. Lepage, 2000. Measuring tree height using scanning laser altimetry, *Proceedings of the 22nd Annual Canadian Remote Sensing Symposium,* 21–25 August, Victoria, BC, Canada (Canadian Remote Sensing Society), pp. 425–432.

(Received 21 October 2002; accepted 18 February 2003; revised 12 March 2003)